Environmental Transformations in Hydrophobicity of TiO_2 P-25 Nanoparticles in Alsea River Waters

By:
Kylie Boenisch

A THESIS

Submitted to:
Oregon State University
Honors College

in partial fulfillment of
the requirements for the
degree of

Honors Baccalaureate of Science in Environmental Engineering
(Honors Associate)

Presented June 4, 2020
Commencement June 2021

AN ABSTRACT OF THE THESIS OF

Kylie Boenisch for the degree of Honors Baccalaureate of Science in Environmental Engineering presented on June 4, 2020. Title: Environmental Transformations in Hydrophobicity of TiO_2 P-25 Nanoparticles in Alsea River Waters.

Abstract approved:_____

Stacey Harper

Hydrophobic titanium dioxide (TiO_2) nanoparticles (NPs) are prevalent in industry and manufacturing. They are known for their white pigmentation, are found in sunscreens, paints, cosmetics, and are frequently used in wastewater treatment. Understanding the physicochemical properties of TiO_2 P-25 NPs, such as hydrophobicity, are essential when determining their fate, transport, and impact in natural systems. Standard methods of testing hydrophobicity (i.e. contact angle or octanol water partitioning) are ineffective for NPs. Dye binding assays with hydrophilic and hydrophobic dyes may offer an effective alternative comparable to K_{ow}; through the ratio of linear adsorption slopes (β), β(hydrophobic dye)/(hydrophilic dye).

Four water samples from varying locations along the Alsea River were collected and incubated with TiO_2 P-25 NPs. A dye assay utilizing known hydrophilic (Nile Blue) and hydrophobic (Rose Bengal) dyes was used to characterize the hydrophobicity of the NPs after incubation. It was found that TiO_2 P-25 NPs, which are known to be hydrophobic in ultrapure water, are hydrophilic in brackish wasters close to the coast. Significant differences in TiO_2 P-25 NP hydrophobicity ($p \leq 0.05$) were observed after incubation in all four water samples when compared to Milli-Q water results.

Key Words: TiO_2 P-25 nanoparticles, hydrophobicity, environmental transformations

Corresponding e-mail address: kylieboenisch1@gmail.com

Environmental Transformations in Hydrophobicity of TiO_2 P-25 Nanoparticles in Alsea River Waters

By:
Kylie Boenisch

A THESIS

Submitted to:
Oregon State University
Honors College

in partial fulfillment of
the requirements for the
degree of

Honors Baccalaureate of Science in Environmental Engineering
(Honors Associate)

Presented June 4, 2020
Commencement June 2021

Honors Baccalaureate of Science in Environmental Engineering project of Kylie Boenisch presented on June 4, 2020.

APPROVED:

_____

Stacey Harper, Mentor, representing Chemical, Biological, and Environmental Engineering

_____

Bryan Harper, Committee Member, representing Environmental and Molecular Toxicology

_____

Susanne Brander, Committee Member, representing Environmental and Molecular Toxicology

_____

Toni Doolen, Dean, Oregon State University Honors College

I understand that my project will become part of the permanent collection of Oregon State University, Honors College. My signature below authorizes release of my project to any reader upon request.

_____

Kylie Boenisch, Author

Acknowledgements:

Thank you to the Harper Laboratory for two years of invigorating research experience, a plethora of opportunities for growth as a researcher, and for being a family to me. Thank you to Mackenzie Johnson for help collecting natural water samples, and for editing many abstracts and the manuscript itself. Additionally, thank you to Dr. Lauren Crandon for allowing me the opportunity to take ownership of the environmental transformations portion of this project, and for providing support and thoughtful feedback throughout this process.

Finally, thank you my parents and sister, my aunt and uncle, my partner, and my extended family and friends who have constantly supported me throughout my time at OSU.

Contribution of Authors

Dr. Lauren Crandon played an integral role developing the dye assay methodology used to determine the hydrophobicity of nanoparticles. She first investigated the application of traditional methodologies like octanol-water partitioning and hydrophobic interaction chromatography, for determining the hydrophobicity of NPs. Limited success in these traditional methodologies led to the investigation of dye adsorption assays, and the eventual development of the dye assay utilized in this thesis. Dr. Crandon also served as a sounding board for the methods development of the environmental transformation application of the dye assay. Finally, Dr. Crandon completed a substantial portion of the literature review and writing of the manuscript, particularly regarding the development of the dye assay methodology.

Dr. Stacey Harper assisted with the literature review, methods development, the delivery of experiments, and manuscript editing. Additionally, Dr. Harper assisted with poster and presentation development for this thesis.

Bryan Harper provided valuable guidance on methods development, the delivery of experiments, assisted with statistical analysis and data processing, literature review, and manuscript editing. Bryan also provided substantial feedback on poster design, and content for the development of this thesis.

The expertise and advice of Dr. Crandon, Dr. Harper, and Bryan Harper were integral to the successful delivery of this project.

Introduction

The work and results of this thesis are presented herein through the manuscript entitled *Adaptive methodology to determine hydrophobicity of nanomaterials in situ*, which was recently published in PLOS One. This manuscript investigates a variety of methods for determining NP hydrophobicity using of CuO, Au, SiO_2, and Ami-SiO_2 NPs. It also presents the application of a dye assay methodology to track environmental transformations in hydrophobicity in natural systems. This document provides the context and methodologies utilized to determine the environmental transformations in hydrophobicity of TiO_2 P-25 nanoparticles after simulated release into Alsea River waters and comprehensively summarizes the results of the work relevant to this thesis.

The dye assay methodology for determining the hydrophobicity of nanoparticles from *Adaptive methodology to determine hydrophobicity of nanomaterials in situ* was used to track the environmental transformation of TiO_2 P-25 NPs after incubation in Alsea River waters. This dye assay functions as an indicator of NP hydrophobicity through the adsorption of known hydrophilic (Nile Blue) and hydrophobic (Rose Bengal) dyes onto NP surfaces. A spectrophotometer was used to determine change in adsorbance at wavelengths unique to each dye, to determine the extent of dye binding to the NP. Since TiO_2 is known to be photocatalytic, preliminary experiments using the dye assay were completed in both the light and the dark. There were significant differences in dye assay results ($p \leq 0.05$) between the light and dark, thus all subsequent experiments were completed in the dark.

For application in collected natural waters, the dye assay procedure was slightly modified to include NP incubation in natural waters, followed by NP resuspension in Milli-Q water. The NPs were resuspended in Milli-Q water to avoid potential precipitation of Nile Blue dye from

salts present in natural water samples. In-depth methods can be found in the "Environmental Transformations" section of *Adaptive methodology to determine hydrophobicity of nanomaterials in situ.*

Relative hydrophobicity is an informative parameter when modeling the fate and transport of nanoparticles after release into the environment. Hydrophobicity is a powerful predictor for determining a particle's partitioning behavior in available environmental compartments like soil, air, and water, bioavailability, and transport in aqueous solutions (1). For example, hydrophilic NPs are more likely to remain suspended in aqueous solutions, while hydrophobic NPs are more likely to sorb to available organic material. Additionally, it is known that hydrophobic NPs experience heightened cellular uptake compared to hydrophilic counterparts through lipid bilayer interactions (2,3).

While this assay is applicable to laboratory settings, its application in the natural world provides powerful insight on the ultimate fate of NPs in natural systems. Thus far, the commercial application of nanoparticles has outpaced extensive research on potential transformations in their physicochemical characteristics impacting their fate and transport, and associated exposure, uptake and toxicity after release into natural environments. This study, which highlights the stark difference in nanoparticle hydrophobicity between laboratory and natural settings, aims to close this gap in knowledge.

TiO_2 P-25 nanoparticles were chosen due to their widespread use and prevalence in industry and manufacturing (4). These NPs are found in sunscreens, paints, cosmetics and are employed in wastewater treatment, making their release into the environment inevitable (4). Additionally, TiO_2 P-25 NPs presented as strongly hydrophobic in ultrapure water, which provided a baseline for highlighting environmental transformations. The Alsea River (Oregon)

was chosen for simulated release because it provided a gradient of water salinities and a variety of ecosystems. Four water samples were collected along the river, starting with fresh headwaters and ending with estuarine waters near the Pacific Ocean. Sample locations included Clemens Park, Mill Creek Park, Tidewater, and Waldport Bay (Fig. S5.). Analyzing the hydrophobicity of TiO_2 P-25 NPs after incubation in each of the water samples allowed for preliminary conclusions to be drawn about the impact of varied river environments on their fate and transport through the lens of hydrophobicity.

Adaptive methodology to determine hydrophobicity of nanomaterials *in situ*

Lauren E. Crandon[1], Kylie Boenisch[1], Bryan J. Harper[2] and Stacey L. Harper [1,2,3]

[1]School of Chemical, Biological and Environmental Engineering, Oregon State University, Corvallis, Oregon, United States of America

[2]Department of Environmental and Molecular Toxicology, Oregon State University, Corvallis, Oregon, United States of America

[3]Oregon Nanoscience and Microtechnologies Institute, Corvallis, Oregon, United States of America

*Corresponding author.

Email address: stacey.harper@oregonstate.edu (SLH)

Introduction

Despite increasing commercial and industrial use of nanoparticles (NPs) in areas such as sunscreens, cosmetics, catalysts, pigments, and antimicrobials, little is known of their environmental impact (5). Estimates predict a rise in global consumption of nanomaterials from approximately 308,322 metric tons in 2016 to 733,220 metric tons in 2021 (6). At their end-of-life, NPs are released and encounter dynamic and complex environments that transform their surface. Currently there is not sufficient information to establish predictive structure-activity relationships for risk assessment, mostly due to lack of physicochemical characterization of nanomaterials in relevant conditions (7). Distribution coefficients are widely used to model the environmental fate and bioavailability of chemicals, but parallel descriptors for nanomaterials have not been widely implemented (8).

One of the most accurate and useful descriptors of chemicals is relative hydrophobicity. Hydrophobicity is an important parameter in risk assessment that can be used to predict movement through soil, transport in aqueous environments, bioavailability to organisms and partitioning in physiological systems (1). Hydrophobicity is also thought to be a key parameter for the prediction of environmental behavior and biological interactions of nanomaterials (9,10). As with chemicals, hydrophilic NPs are more likely to remain in the water column and potentially have increased mobility, whereas hydrophobic particles are more likely to attach to sediment organic matter. In addition, surface adsorption, which is expected to be dictated in part by hydrophobic interactions, is a primary factor determining NP interactions in the environment (11). When NPs enter the environment, they encounter environmental constituents such as natural organic matter (NOM), ions and polysaccharides, which adsorb to the NP surface and form a dynamic corona, altering the NP surface properties and influencing fate, transformations,

and uptake (12). The surface hydrophobicity of NPs likely influences the composition of the corona and affinity for the surrounding environmental surfaces (13).

This concept is further applied to describe the interaction of NPs with organisms. Hydrophobic NPs have shown to interact with the lipid bilayer of organisms, and evidence suggests increased uptake relative to hydrophilic NPs (2). After uptake, NP surface hydrophobicity has been shown to directly affect toxicity, circulation time, and bioaccumulation (14,15). Additionally, hydrophobicity dictates interaction of the NP surface with biological components such as proteins and biomolecules which adsorb to the surface, further altering biological interaction (16).

Nanoparticle-specific considerations add to the complexity of measurement and interpretation of hydrophobicity metrics. NPs can be comprised of various sizes and surface functionalization, both of which affect partitioning behavior and interactions. Hou *et al.* found that the size of Au NPs affected how quickly NPs distributed to a solid-supported lipid membrane, while surface functionality and solution chemistry determined the "apparent" steady state concentrations (17). Agglomeration can also affect fate and complicate measurements by causing settling of NPs over time and preventing true partitioning behavior (18). NPs are often functionalized with various surface coatings which can also alter surface hydrophobicity. Previous studies have found that changes in hydrophobicity of the particle surface can alter cell interactions and consequent uptake (19). Another study found that the attachment of Ag NPs to hydrophobic collector surfaces was directly proportional to hydrophobicity of coatings (citrate, PVP, and GA) (20). Therefore, a useful measure of hydrophobicity is needed that accurately represents complex and dynamic NP behavior.

Traditional methods to quantify the hydrophobicity of chemicals and solid surfaces rely on partitioning or other equilibrium dependent measurements. However, NPs do not reach thermodynamic equilibrium, so kinetically controlled parameters are more relevant and appropriate (21). One approach is to obtain values for attachment efficiency (α) of NPs which can be directly applied to model the deposition of NPs to a collector surface as using the Smoluchowski equation. This method is well established for modeling the coagulation of particles and has been shown to successfully quantify the attachment of certain NPs to surfaces in complex environments (22–26). However, α must be experimentally determined for each pair of surfaces and is dependent on media properties such as ionic strength, pH, and concentration of organic matter. There is a need to quantify the inherent surface hydrophobicity of NPs to predict attachment to surfaces using computational fate models in a manner parallel to forecasting the partitioning of chemicals into environmental compartments.

Existing methods for characterizing the hydrophobicity of substances have been applied to NPs and met with varying degrees of success. Examples of these methods include contact angle, which is typically used to evaluate the hydrophobicity of solid surfaces, octanol-water partitioning, which is commonly used for chemicals, and hydrophobic interaction chromatography, which provides a relative measure of the hydrophobicity of proteins. In some cases, these methods have been modified for NP specific behavior.

Contact angle measures the wettability of a solid surface by a probe liquid, typically using the sessile drop technique, and measuring the angle at the solid-liquid-vapor interface. To apply this technique to nanomaterials, a NP suspension is first filtered and pressed into a flat disk before applying the probe liquid. This method was performed across a series of rare earth oxide NPs and all were found to be hydrophobic, with water contact angles between 100° and 115°

(27). A similar method was applied to fullerenes, fullerols and coated Ag NPs at the liquid, liquid, solid interface and all were found to be hydrophilic, which was inconsistent with other measurements (28). Arnaudov *et al.* used a gel trapping technique to eliminate the need to press NPs into a flat disk, but this method requires advanced techniques such as atomic force microscopy and does not consider effects of agglomeration or functionalization (29). A major limitation of using contact angle for hydrophobicity is that it does not allow for experimental *in situ* measurements (27,28,30). Additionally, it does not take into account NP size, shape, surface roughness, or heterogeneity (31).

If NP suspensions are modeled as homogenous solutions, the partitioning behavior between two immiscible liquid phases (octanol and water) could be used to evaluate hydrophobicity. The octanol-water partitioning coefficient (K_{OW}) is commonly used for chemicals and is a powerful descriptor to model environmental fate and bioavailability for risk assessment (32). Octanol is used as a surrogate for organic rich material, such as the sediment or lipid membrane. This measurement, when applied to dissolved chemicals, assumes that solutes move freely between two phases, and the equilibrium concentrations represent the "affinity" for each phase.

NP suspensions violate the basic assumptions of solubility and equilibrium associated with K_{OW}, but many studies still apply this measure to evaluate the hydrophobicity of NPs (21). The method has been most commonly applied to fullerenes, and although they are generally characterized as very hydrophobic, exact values are not consistent among studies and span orders of magnitude (28,33). When applied to carbon nanotubes, measured K_{OW} values were not found to be predictive of bioaccumulation in earthworms or oligochaetes. The K_{OW} of nanomaterials

has been reported to be inconsistent with organic compounds of a similar chemical structure, with aggregation, size and surface coatings all being cited as possible explanations (34).

Some studies have attempted to obtain a K_{OW} value for NPs while acknowledging the shortcomings or making efforts to adapt the results for particle-based systems. When applying the shake-flask method to measure K_{OW}, some nanomaterials have been observed to partition at the interface between the aqueous and octanol phases. A two parameter distribution coefficient was proposed to analyze measurements in this scenario, where the mass ratio of NPs in the aqueous, organic, and interface are all taken into account (35). The resulting measurements are system-dependent and a function of area of the interface, particle count, and time. Another proposed adaptation is to evaluate the K_{OW} of the surface functional groups alone, and assume that the core has a negligible effect on surface hydrophobicity (10). This is likely most suitable for NPs with small cores and large, branched organic coatings. K_{OW} measurements of this nature may be useful to compare within a class of nanomaterials but have not been widely implemented to date.

An alternative method to evaluate hydrophobicity of NPs is hydrophobic interaction chromatography (HIC). HIC is typically used to separate proteins based on their relative hydrophobicity (36). Proteins are eluted through a column by a stepwise decrease in salt concentration, where the most hydrophobic proteins are eluted at the lowest salt concentration. The stationary matrix of the column is typically comprised of agarose beads functionalized with alkyl chains of various lengths. While this method is potentially suitable for application with NPs due to the similar size range of proteins, it has only been applied to measure hydrophobicity of NPs in a limited number of studies. Polystyrene NPs were evaluated at a constant salt concentration and the elution volume required to completely remove particles from an alkyl-

agarose column was used as a measure of hydrophobicity (37). Another adaptation was to use multiple columns with varying alkyl chain lengths to compare hydrophobicity of various polymeric NPs (38). HIC can potentially be used for particles with a wide range of hydrophobicity because the stationary phase can be selected by the user.

The adsorption of hydrophobic dyes to the particle surface is another method that is potentially well suited to NPs. This method has been applied to fluorescently labeled polystyrene NPs, latex particles with various functional groups, and solid lipid NPs using Rose Bengal, an organic dye, as a hydrophobic probe (19,39,40). Some difficulties identified with this method were interference from surfactants, time intensive range-finding for suitable NP concentrations, and difficulty separating NPs from suspension for absorbance analysis. Rose Bengal provides robust measurements for hydrophobic NPs but provides limited information about hydrophilic surfaces. A hydrophilic dye, Nile Blue, has been proposed as a means to provide resolution to measurements of hydrophilic particles (28). The use of both hydrophobic and hydrophilic dyes is promising to provide measurements with good resolution to compare NPs with a wide range of compositions.

In this study, we evaluated HIC and dye adsorption (Rose Bengal and Nile Blue) to evaluate the hydrophobicity of NPs and compared them to traditional K_{OW} methods. The results were evaluated based on the ability of each method to overcome major challenges associated with NPs: agglomeration and surface functionalization. Uncoated gold (Au) NPs were selected for their small size and ability to be easily quantified by absorption spectroscopy. Uncoated copper oxide (CuO) NPs were used for their known propensity to agglomerate in solution. Silica (SiO_2) NPs with and without amine surface functionalization were chosen to evaluate the ability of the methods to observe changes in hydrophobicity due to surface coatings. We adapted

protocols to improve use for widespread applicability to NPs, with the ultimate goal of obtaining useful measurements for future environmental fate models. TiO_2 NPs, which are prevalent in industry and manufacturing were used to illustrate the application of the dye adsorption methodology in natural settings, tracking a transformation in hydrophobicity in natural waters, providing a power tool for future modeling.

Methods

Nanoparticle preparation

Stock suspensions (1000 mg/L) of 14 nm Au (U.S. Research Nanomaterials, Inc. Houston, TX), CuO (<50 nm, Sigma Aldrich), 80 nm SiO_2 and aminated SiO_2 (NanoComposix, San Diego, CA) NPs were prepared in 20 mL ultrapure water (MQ, Milli-Q 18.2 Ω resistivity, Merck Millipore, Burlington, MA) and sonicated with a cup horn style sonicator equipped with a circulating water bath to maintain temperature (Vibracell VCX 750, Sonics & Materials, Inc., Newtown, CT) at 40% amplitude for 2 minutes (40.1 W, 4812 J). Stocks were further diluted in ultrapure water.

Nanoparticle characterization

The hydrodynamic diameters (HDD) of CuO, Au, SiO_2, and Ami-SiO_2 NPs were evaluated in ultrapure water immediately following dispersion and sonication. A volume of 1.5 mL was placed in a disposable cuvette for measurement. Zeta potential measurements were performed in 0.5x phosphate buffered saline (PBS) to provide sufficient ionic strength to carry an electrical charge. HDD and ZP measurements were both performed using a Malvern Zetasizer (Nano ZS, Malvern Instruments, Worcestershire, UK) and the detailed parameters are described in Table S1.

Octanol-water partitioning

The OECD shake flask method (41) was applied to obtain a K_{OW} value for Au NPs. A volume of 4 mL each of ultrapure water and 1-octanol were equilibrated for 24 hours with 0.2 mg Au NPs. The liquid phases were allowed to separate for 4 hours, after which samples were collected from each phase and Au NPs were quantified using a SpectraMax M2 spectrophotometer (Molecular Devices, Sunnyvale, CA, USA) at λ= 530 nm. Absorbance was converted to concentration using a standard curve prepared in ultrapure water or 1-octanol. The same method was used to evaluate CuO NPs except the absorbance was evaluated at 640 nm.

Hydrophobic Interaction Chromatography

HiTrap Octyl FF prepacked HIC columns were purchased from GE Life Sciences (Piscataway, NJ). The bed volume was 1 mL and the stationary phase consisted of a sepharose support matrix of 90 µm beads functionalized with hydrophobic octyl ligands, which were selected to parallel the octanol reference phase of the K_{OW} method. The column was loaded with 2 mL of a 10 mg/L Au NP suspension at a flow rate of 1 mL/min. A lower concentration was used (10mg/L) relative to the K_{OW} method to limit agglomeration, which would block flow through the pore space. After loading the column, a syringe pump (Model No. NE-1010, New Era Pump Systems, Inc. Farmingdale, NY, USA) was used to flow 20 mL of 0.5x PBS through the column at 1 mL/min and the eluent was collected in 1 mL fractions. To remove Au NPs retained in the column during PBS elution, a surfactant (0.1% Triton X-100, laboratory grade, Sigma-Aldrich, St. Louis, MO), was pumped through the column at 1 mL/min for another 20 minutes, and the eluent was again collected in 1 mL fractions every minute. The collected samples from both elution phases were placed in a 96-well plate and the absorbance at 530 nm was evaluated using UV-vis spectroscopy to determine Au concentration.

Dye Adsorption

The relative adsorption of a hydrophobic probe (Rose Bengal, 85% ACROS Organics, New Jersey, USA) and a hydrophilic probe (Nile Blue A, ACROS Organics, New Jersey, USA) to the NP surface was used as a measure of hydrophobicity (Fig 1). Dye concentrations (0.5-30 μM) were prepared in ultrapure water. Equal volumes of dye and NP stock were combined in 1.5 mL microcentrifuge tubes for each concentration and incubated in a tube rotator for 90 minutes. Controls were prepared by adding dye to ultrapure water to account for any observed loss of dye due to adsorption to the vials. To evaluate potential degradation of dye by reactive oxygen species (ROS) from the NP surface, controls were prepared with various concentrations of H_2O_2. Each sample was prepared in triplicate. Following incubation, NPs were removed from solution by centrifugation for 30 minutes at 14000 rpm. The remaining concentration of dye in the supernatant was analyzed using UV-Vis spectroscopy at λ= 543 nm for Rose Bengal and λ= 620 nm for Nile Blue. This method was performed with final concentrations of 500 mg/L SiO_2 and Ami-SiO_2 and 250 mg/L CuO. The dye concentrations were selected based on the minimum and maximum detectable absorbance by the UV-Vis spectrometer. NP concentrations were maximized to observe a significant change in absorbance while minimizing the effects of agglomeration. A lower CuO concentration was used to minimize agglomeration.

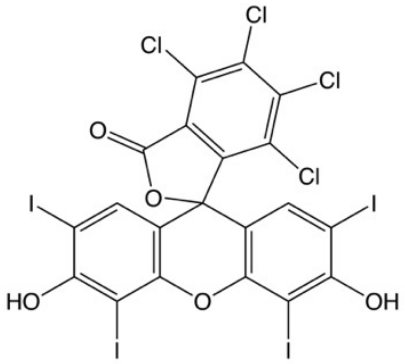

Rose Bengal

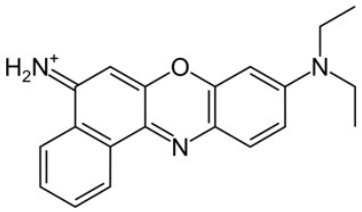

Nile Blue

Fig 1. Structures of the hydrophobic (Rose Bengal) and hydrophilic (Nile Blue) probes.

The amount of dye adsorbed to the NP surface (q_e) was calculated using Eq. 1:

$$q_e = (C_0 - C_e)\frac{V}{m} \quad (1)$$

where C_0 is the initial dye concentration, C_e is the concentration of dye reaming in the supernatant after centrifugation, V is the volume (L) and m is the mass of NPs (g). The adsorption of dyes was fit to a linear (Eq. 2), Langmuir (Eq. 3) and Freundlich (Eq. 4) type isotherm models. Each model was fit by minimizing the sum of squared errors in SigmaPlot (Systat Software, San Jose, CA, USA) to determine the linear adsorption constant, k_{lin} (L/g), the adsorption capacity, q_{max} (μmol dye/gNP), the Langmuir adsorption capacity, K_f (L/umol) and the adsorption intensity, 1/n for the Freundlich model.

$$q_e = k_{lin}C_e \quad (2)$$

$$q_e = \frac{q_{max}K_L C_e}{(1+K_L C_e)} \quad (3)$$

$$q_e = K_f q C_e^{1/n} \quad (4)$$

Environmental transformations

To simulate the environmental release of NPs and evaluate the effect on dye adsorption, natural water samples were collected from various sources along the Alsea River Watershed in Oregon (Fig S5). Conductivity and pH were measured at the time of collection. The samples were later filtered using a 0.44 mm Whatman GF/F glass fiber filter to remove particulate matter prior to performing alkalinity and hardness tests. Suspension of TiO_2 NPs (250 mg/L) were prepared in each of the water samples and allowed to incubate for 90 minutes. NPs were then removed by

centrifugation and resuspended in ultrapure water, after which the previously described method for dye adsorption was performed. To perform HDD and zeta potential measurements, 10 mg/L TiO_2 NPs were incubated in natural water sources; measurements were then taken using a Malvern Zetasizer (Nano ZS, Malvern Instruments, Worcestershire, UK). To avoid photocatalytic activity from TiO_2, all experiments regarding environmental transformations were completed in the dark.

Statistical Analysis

SigmaPlot version 13.0 (Systat Software, San Jose, CA, USA) was used to perform all statistical analyses. All experiments were performed in triplicate. Area under the curve (AUC) measurements for HIC analysis were performed in SigmaPlot using built in graphical integration functions.

Results and Discussion

Nanoparticle characterization

Au, SiO_2, and Ami-SiO_2 NPs were all stable in suspension and had an average HDD of 76.8 ± 1.5 nm, 100.3 ± 0.3 nm, and 113.5 ± 0.5 nm in ultrapure water, respectively, which is similar to their primary particle size (Fig 2A). CuO NPs showed a high degree of agglomeration, with an average HDD of 556 ± 87 nm in ultrapure water compared to a primary particle size of <50 nm. Agglomeration is expected to be more significant in complex media such as the 0.5x PBS buffer used for zeta potential measurements (42). The ZP of the CuO NPs was -31.7 mV, indicating that despite high agglomeration, the suspension was stable. The zeta potential shows that all particles had a negative surface charge in 0.5x PBS (Fig. 2B). The surface charge of Ami-SiO_2 was neutralized relative to SiO_2. The isoelectric point of Ami-SiO_2 is pH 7.5 compared to 2.5 for SiO_2, so below this pH the surface would be expected to be positively charged. The pH of the PBS solution was approximately 7.8.

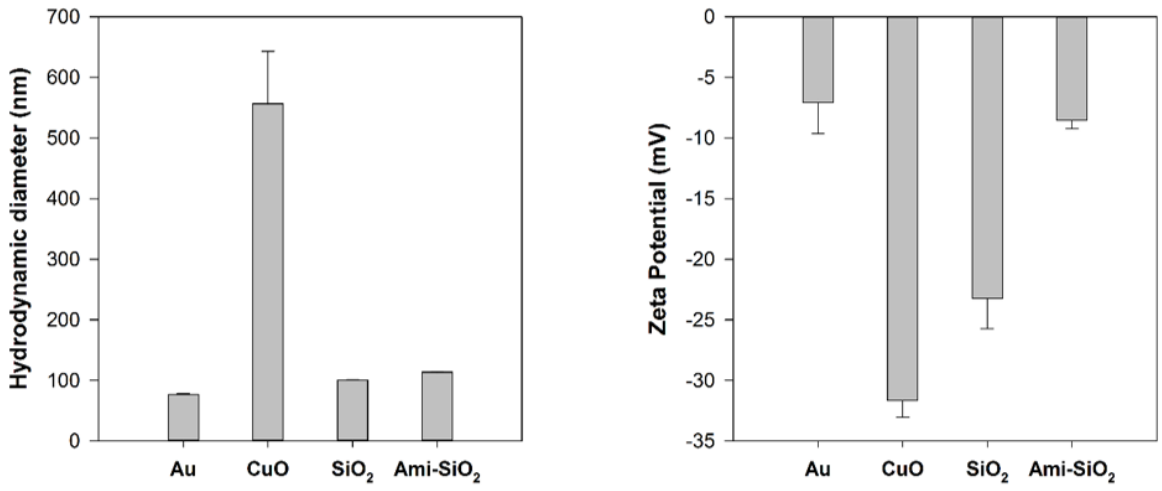

Fig 2. Hydrodynamic diameter of Au, CuO, SiO_2, and Ami-SiO_2 evaluated in ultrapure water and zeta potential evaluated in 0.5x PBS.

Octanol water partitioning (K_{OW})

Au and CuO NPs were selected to evaluate octanol-water partitioning because the particles can be easily quantified using UV-Vis spectroscopy. Au particles partitioned to the aqueous phase and remained suspended (Fig. S1). No visible Au NPs were observed at the octanol-water interface. A log K_{OW} of approximately -2.1± 0.6 was calculated, suggesting Au NPs are hydrophilic.

The log K_{OW} of Au NPs measured in this study was compared to published values for Au, and it was found that the reported hydrophobicity of elemental gold is not consistent among studies. Native gold flakes were found to be hydrophobic and floated in water (43). However, Smith *et al.* performed a comprehensive review of studies that characterized the contact angle of Au and found opposing conclusions about its hydrophobic or hydrophilic nature. Performing

Auger electron spectroscopy before and after each measurement revealed that organic impurities were causing hydrophobic measurements, and clean gold surfaces were determined to be inherently hydrophilic (44). The modeled value of log K_{OW} for elemental Au was found to be slightly hydrophobic (log K_{OW} Au = 0.03), while ionic forms were hydrophobic (Log K_{OW} $AuCl_3$ = 0.16) or hydrophilic (log K_{OW} AuCl = -0.46) depending on the valency (45).

CuO NPs were visually observed to aggregate at the liquid-liquid interface and settled to the bottom of the vial over time (Fig S2). Additionally, CuO in the octanol phase could not be accurately quantified because they did not disperse in octanol (Fig S3). The measured log K_{OW} was -0.34 ± 0.39. Modeled log K_{OW} values of the bulk and dissolved phases were estimated to be -1.10 for CuO, 0.52 for $CuCl_2$, and 0.16 for elemental copper (45). This is consistent with experimentally determined contact angle measurements of Cu films, which showed a change from slightly hydrophobic to slightly hydrophilic as the surface oxidized to CuO (46). CuO is known to exhibit some dissolution of Cu^{+2} in aqueous systems which may also affect the hydrophobicity at the surface (47).

Despite some limited success in this study and others, the octanol-water partitioning method cannot be widely applied across classes of NPs or systems and should be limited to comparisons among classes of NPs. The overall conclusion of hydrophobic or hydrophilic was in agreement with other measures of hydrophobicity in the literature, so this method may be useful as a preliminary qualitative observation, but measured values do not provide sufficient resolution or consistency for use in fate models. NP suspensions do not reach a thermodynamic equilibrium between liquid phases, and values for K_{OW} are dependent on NP concentration, time, and size of the vial which affects the area of the liquid-liquid interface. This was particularly evident for CuO NPs, which exhibit significant agglomeration and settling.

Hydrophobic Interaction Chromatography

The HIC method was adapted to measure hydrophobicity of NPs by interaction with hydrophobic octyl ligands. Salt concentration was not varied, and instead mass of particles retained in the column was compared to mass of particles eluted by an aqueous phase (0.5x PBS). Concentration of Au plotted as a function of cumulative eluent volume (Fig 3) shows that a high concentration of Au NPs was initially flushed out in the first column volume, which was likely residual from the loading step. Small concentrations of Au NPs were measured in the eluent throughout the PBS phase. Some Au NPs were initially eluted with the surfactant but those particles only represented a small portion of Au retained in the column. The concentration of Au retained in the column was difficult to determine by UV-Vis analysis because of interference from the surfactant bubbles, so higher variance was therefore observed in this elution phase relative to the PBS phase (Fig 3). Degassing the mobile phase under vacuum may minimize this problem for future studies.

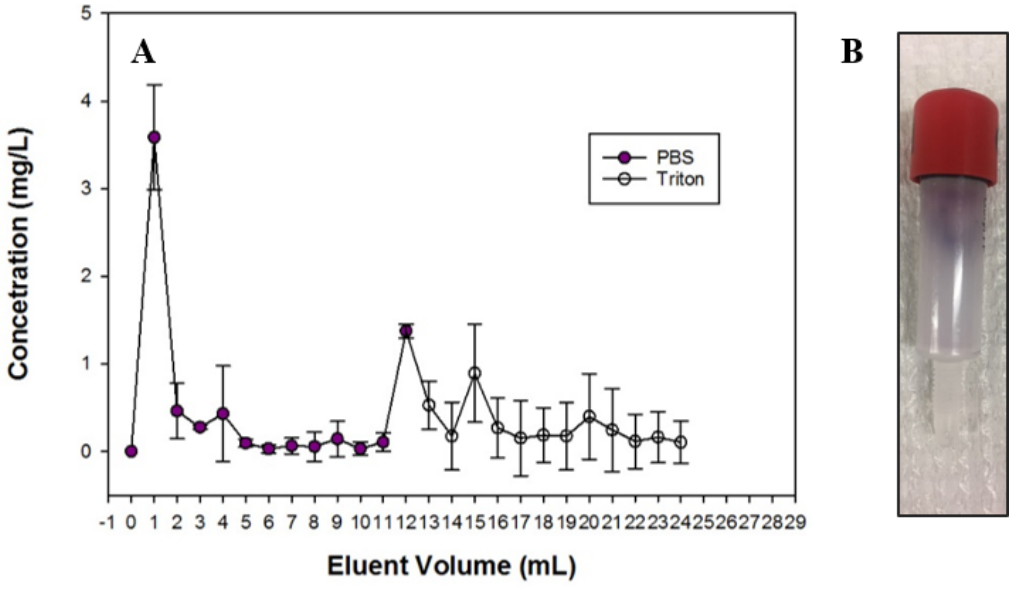

Fig 3. A) Concentration of Au in the eluent with PBS and Triton mobile phases as a function of total eluent volume. B) Gold NPs visibly retained in column after flushing with 20 mL surfactant and 20 mL 20% ethanol.

For analysis, the area under the curve (AUC) of concentration vs. volume was evaluated to determine total Au mass in the PBS and surfactant eluents. The ratio was used as a measure of hydrophobicity according to Eq 5:

$$LogK_{OW,HIC} \cong \frac{AUC_{surfactant}}{AUC_{PBS}} \quad (5)$$

Log $K_{OW,\,HIC}$ for Au NPs was calculated to be -0.447 ± 0.006, indicating they are hydrophilic.

Although the HIC method is rapid, directly comparable to log K_{OW}, and potentially more appropriate for nanomaterial behavior, several factors limit its widespread use. Au NPs were not fully recovered from the column, and their size likely restricted travel through the pore space. Particles were visually observed to be retained at the top the column, even after flushing with 20 mL surfactant and further attempts to regenerate the column with 20 mL 20% ethanol (Fig. 3B). Previous studies have also observed higher rates of NP column retention than predicted by classical filtration theory, which models interaction of a single particle with a collector surface, with deposition governed by DLVO forces (electrostatic and Van der Waals) (48). Chowdhury et al. observed an increase in retention of TiO_2 NPs in sand columns with increased agglomeration, despite unfavorable electrostatic interactions (49). This was attributed to straining, which refers to physical retention in the pore structure, and has been reported to occur when the ratio of NP diameter to bead diameter is greater than approximately 0.002 (50). In this study, the ratio of the primary particle size (14 nm) to bead diameter (90 µm) is 0.00016, but using the aggregate size the ratio is 0.0009. Straining likely plays a role in the observed column retention, and would

certainly be more severe for particles with more significant agglomeration, such as metal oxides, but may not be the only explanation. Alternative reasons for high retention include charge heterogeneity of the stationary phase and the presence of organic impurities (48).

Theoretically, the columns can ideally be regenerated, but we were unable to completely remove particles after loading. In addition, it was difficult to accurately quantify NPs in the eluent. UV-Vis spectroscopy is simple and widely available, but many NPs may have absorbance interference with plates or cuvettes, and concentrations in this case were too low for sensitive quantification. Absorbance was not a reliable measure in the surfactant eluent due to interference from bubbles forming in solution. Other methods may be more suitable, such as inductively coupled plasma mass spectrometry (ICP) for metal particles, nanoparticle tracking analysis (NTA) for stable and spherical particles, or other analytical methods for carbonaceous NPs but these are more costly and less accessible.

We were unable to perform HIC due to difficulties in recovering and quantifying NPs concentration in the eluent. Columns with larger pores may improve the usefulness of this method. Salt concentrations can be increased or decreased to alter hydrophobic interactions within the stationary phase. The column stationary phase can be selected to be functionalized with alkyl ligands of various chain lengths, and a lower degree of ligand substitution could also decrease the retention of particles in the column. However, this would be less comparable to K_{OW} and these parameters would need to be optimized for specific nanomaterials.

Dye Adsorption

The dye adsorption method was successfully performed for agglomerated and functionalized particles. Adsorption isotherms were fit to linear, Langmuir and Freundlich models (Table 1). Linear models can generally be applied at low adsorbate concentrations (51).

The Langmuir model assumes monolayer adsorption on a relatively regular surface (52). The Freundlich model describes adsorption on a heterogeneous surface. In general, the data were best represented by the linear and Freundlich models (Table 1). The linear adsorption constant, k_{lin}, was used as a measure of affinity for each probe to the NP surface. The relative affinity of RB and NB to the surface was evaluated and then Eqn. 6 was used as a unitless measure of hydrophobicity, shown here as a hydrophobicity ratio (HR).

$$LogHR_{RB/NB} = Log\ \frac{k_{lin,RB}}{k_{lin,NB}} \quad (6)$$

Previous studies that used RB adsorption to measure hydrophobicity of NPs varied the NP concentration and held the dye concentration constant, plotting fraction of dye adsorbed (known as the partition quotient) as a function of surface area (28). We adapted these methods and instead plotted adsorption isotherms by varying the dye concentration and using a constant NP concentration. This eliminates the need to calculate NP surface area, which is difficult to measure *in situ* and can contribute to uncertainty in measurements. Additionally, this reduces NP waste and simplifies preliminary range finding for optimizing NP concentration. Adsorption isotherms are well established for suspended particles, and do not require assumptions of spherical geometry or monodispersity to estimate surface area.

Table 1. Summary of isotherm parameters

Linear	**CuO**	**SiO_2**	**Ami-SiO_2**
$k_{lin,RB}$	0.090 ± 0.127	0.254 ± 0.044	1.99 ± 0.49
R^2	0.02	0.65	0.67
$k_{lin,NB}$	2.90 ± 0.07	13.23 ± 39.70	0.05 ± 0.02
R^2	0.99	0.86	0.40
Langmuir			
$q_{max, RB}$	3.57 ± 1.13	----	44.13 ± 53.01
$K_{L, RB}$	1.23 ± 1.96	----	0.067 ± 0.10
R^2	0.11		0.68
$q_{max, NB}$	876.86 ± 4944.49	44.81 ± 5.86	2.18 ± 5.77
$K_{L, NB}$	0.004 ± 0.024	0.77 ± 0.20	0.03 ± 0.10
R^2	0.89	0.93	0.41
Freundlich			
1/n, RB	0.53 ± 0.48	---	1.14 ± 0.27
$K_{F, RB}$	1.53 ± 0.50	---	2.16 ± 1.48
R^2	0.02	---	0.67
1/n, NB	0.77 ± 0.03	0.31 ± 0.16	1.49 ± 0.03
$K_{F, NB}$	5.61 ± 0.38	17.06 ± 4.17	0.016 ± 0.001
R^2	0.98	0.97	0.59
Log HR	-1.51	-1.72	1.60

For CuO NPs, both dyes adsorbed to the surface, but NB had higher adsorption than RB (Fig 4). CuO NPs had a high degree of agglomeration (Fig. 2), which can affect the available surface for adsorption. However, this effect is likely similar for both dyes, and is essentially normalized when Eqn. 6 is applied. This suggests that the dye adsorption method can be used for particles that agglomerate in solution.

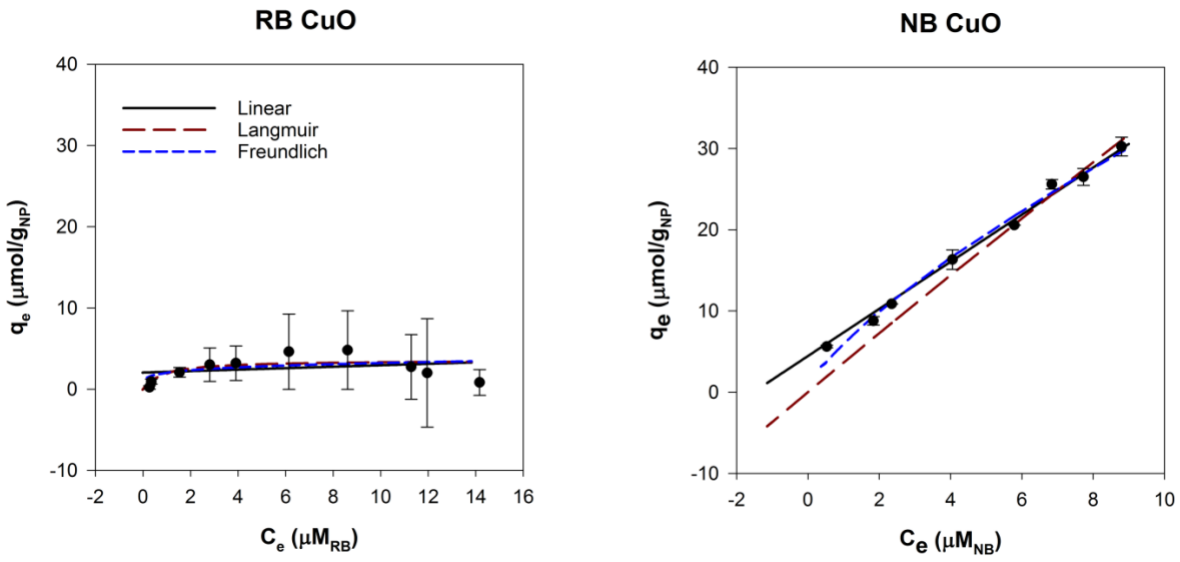

Fig 4. Adsorption isotherms for 250 mg/L CuO with Rose Bengal and Nile Blue modeled with linear, Langmuir and Freundlich adsorption models.

SiO_2 particles with and without amine functional groups were compared using the dye adsorption method (Fig 5). Both have low solubility at pH 2-8 and remained stable in suspension. Bare silica was predicted to be hydrophilic (log K_{OW} is -0.66), which is consistent with our results (45). NB adsorbed to the SiO_2 surface while negligible RB was adsorbed.

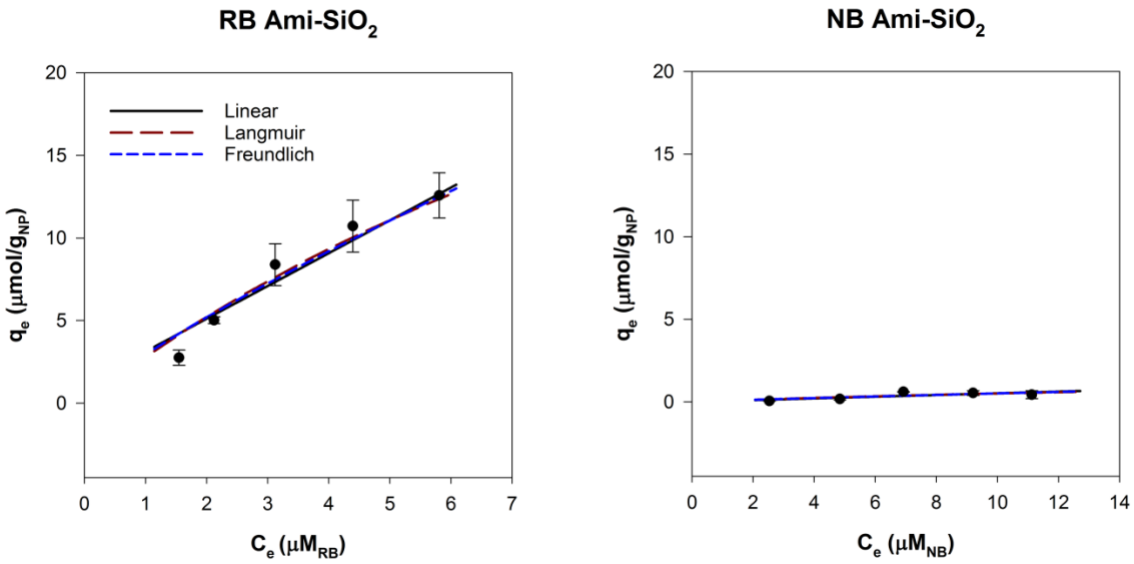

Fig 5. Adsorption isotherms for 500 mg/L SiO_2 NPs with Rose Bengal and Nile Blue, modeled with linear, Langmuir and Freundlich adsorption models.

Amine groups at the surface drastically altered the hydrophobic interactions of the SiO_2 core. Ami-SiO_2 showed the opposite trend of SiO_2 NPs and had high adsorption of RB and minimal NB adsorption (Fig 6). The k_{lin} for RB was 1.99 ± 0.49 and log ($k_{lin,RB}/k_{lin,NB}$) was 1.60. The observed hydrophobic nature is consistent with the log K_{OW} for amine groups, which become more hydrophobic with increasing alkyl chain lengths (45). The results indicate that the dye adsorption method is well suited to evaluate NPs with covalently bound functional groups. This method can measure the change in surface hydrophobicity of NPs due to functionalization and potentially incorporate factors such as size and surface coverage.

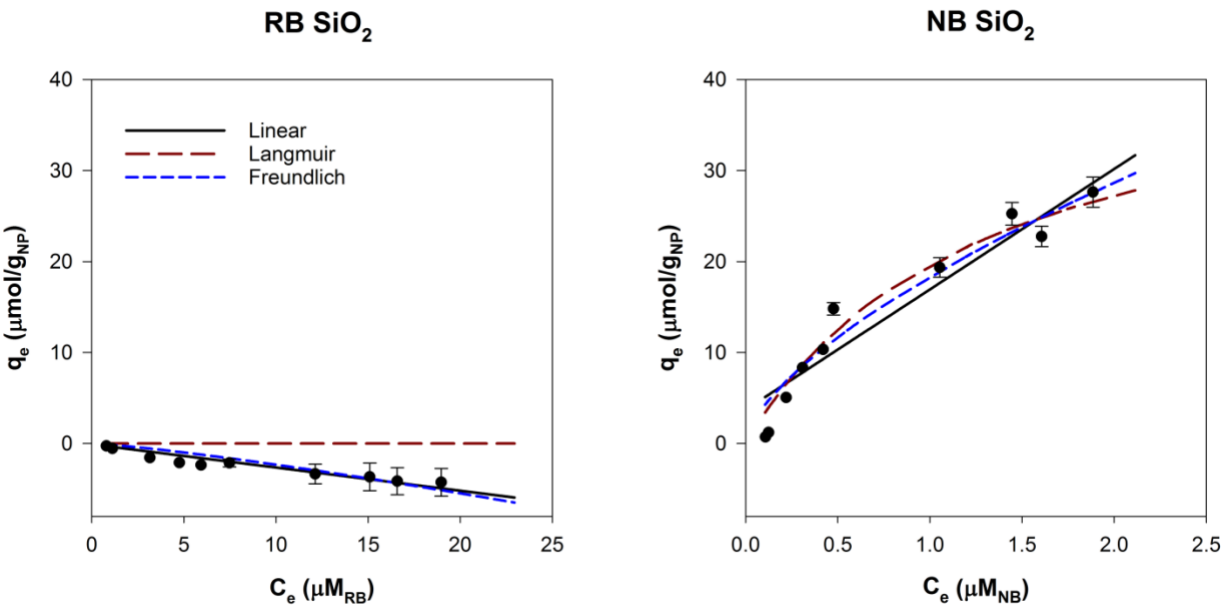

Fig 6. Adsorption isotherms for 500 mg/L Ami-SiO2 NPs with Rose Bengal and Nile Blue, modeled with linear, Langmuir and Freundlich adsorption models.

A potential shortcoming of the dye adsorption method is that it is difficult to distinguish between adsorption due to hydrophobic interaction or due to electrostatic interaction. The probes used here are oppositely charged: RB is anionic and NB is cationic. The Ami-SiO2 NPs had a positively charged surface and therefore likely experienced electrostatic interaction with RB. Amine functionalized mesoporous hollow silica shells were previously found to completely remove another anionic dye, Congo Red, from solution and this was attributed to the oppositely charged surface (53). However, Congo Red is also hydrophobic (log Kow=3.57) which could have contributed to the high rate of adsorption. In the current study, CuO suspensions were negatively charged but adsorbed some anionic Rose Bengal, indicating that despite repulsive electrostatic charges, hydrophobic interactions led to adsorption.

Environmental Transformations

Environmental transformations caused differences in hydrophobicity measurements and can be measured. The transformations were observed even after NPs were removed from the natural water and re-suspended in MQ. Fresh water samples collected along the Alsea River Watershed were used to evaluate potential environmental transformations of NPs. Samples were analyzed (Table S2) and varied mostly in conductivity, with Waldport Bay having the highest (53500 μS). TiO_2 NPs were selected here because they are one of the mostly widely produced engineered NPs, and their use in personal care products makes them likely to be present in surface waters at detectable concentrations (54). The HDD of TiO_2 after 90 minutes of incubation was 1223 nm and 2256 nm when measured in ultrapure and Waldport Bay water, respectively (Table S3). The increase in HDD may have decreased the overall NP surface area available for dye adsorption. The dye assay was performed in all water samples and the linear adsorption parameters are shown in Table S4. When TiO_2 NPs were suspended in natural fresh water, there was greater adsorption of NB in all water sources and less adsorption of RB relative to MQ (Figs S6-S8). Significant differences ($p \leq 0.05$) between both $k_{lin,RB}$ and $k_{lin,NB}$ demonstrated a shift from the hydrophobic nature of TiO_2 NPs observed by high adsorption of RB in ultrapure water. This change is likely due to ions and organic matter which interacted with the NP surface to alter its properties.

Prior to measuring dye adsorption, NPs suspended in natural waters were removed and resuspended in ultrapure water because preliminary studies revealed that high salt concentrations caused NB dye to precipitate out of solution. However, environmental transformations could still be observed even when the assay was performed in ultrapure water. This method is promising to provide a quantitative measure of changes at the NP surface.

Comparison of methods

The major advantages and limitations of the three methods shown here are summarized in Table 2. Most notably, the dye adsorption assay does not require direct quantification of NPs. This is a major advantage because various methods are used to quantify nanomaterials depending on material composition and availability of instruments, and this can lead to inconsistent values among studies. For metal and metal oxide NPs that dissolve in solution, metal ions could interfere with measurements to quantify NPs, particularly in the octanol-water partitioning method. If dissolution is sufficient to alter the local ionic strength, adsorption processes occurring in both the HIC and dye adsorption methods could be affected (55). For the dye adsorption method, an ionic control could be used to account for potential complexes that form between the probe dyes and metal ions.

Table 2. Comparison of methods to evaluate NP hydrophobicity

Method	Advantages	Limitations
K_{OW}	• Simple • Directly comparable to existing measurements and fate models	• Violates equilibrium assumptions • Must directly quantify NPs • Settling of NPs affects measurements • Measurement depends on particle count, area of interface, etc.
HIC	• Rapid • Minimal NP waste	• Movement limited through pore space • Must directly quantify NPs
Dye Adsorption	• Do not have to directly quantify NPs • Suitable for NPs that agglomerate • Does not require extensive range finding • Can be applied in natural systems	• Difficult to interpret if no adsorption • Charged probes contribute to adsorption • Octanol is not reference phase

The dye adsorption method, unlike the other methods, produced meaningful results despite high agglomeration of CuO NPs. This method allows for *in situ* measurements without the need for stabilizing agents and can potentially be applied to evaluate the surface hydrophobicity of NPs in more complex environments. Although the probes selected here may produce measurement artifacts due to opposite surface charges, relative differences between NPs can be observed and alternative probes may be explored in the future. We conclude that dye adsorption is most suitable for broad application with NPs.

Conclusion

Surface hydrophobicity is a key parameter influencing environmental fate and biopartitioning, and a standard metric is needed to compare across NPs. A number of disparate protocols are applied in the literature, depending on the chemistry and stability of the NP suspension. This study surveyed and modified candidate methods to be used as a standard measurement of NP surface hydrophobicity. Measuring the adsorption of hydrophilic and hydrophobic dyes to the NP surface is proposed as the most viable method to broadly compare the hydrophobicity of NPs. When compared to alternative methods currently being employed, we conclude that the dye adsorption assay is the best in terms of ability to overcome difficulties associated with agglomeration, functionalization, and quantification of nanomaterials. In this study, changes in dye adsorption could be observed after suspension of NP in natural waters, providing a possible path forward to quantify complex environmental transformations. The octanol water partitioning method was determined to only be suitable for select particles that are small, stable and easily quantified, limiting its widespread use. HIC is theoretically suitable for future use with NPs but is problematic for agglomerated NPs and would require thorough optimization of a reference column. The dye adsorption method is rapid and can be implemented

to assess the hydrophobicity of broad classes of NPs. It should be further validated with the ultimate objective of application in future predictive fate models.

Acknowledgements

The authors thank Macklin Turnquist for work on dye adsorption method development, Zia Klocke for early work with HIC, Shannon Quinn for work on octanol-water method, Padmaja Chavan for technical work on dye adsorption, Lindsay Denluck and Mackenzie Johnson for thoughtful editing of manuscript.

Supporting Information

Table S1. Standardized information for determining the zeta potential in 0.5x PBS.

Shape	spherical
Model used to compute zeta potential	Henry's Equation (Smoluchowski approximation)
Applied voltage	148 V
Replicate measurements	3
Equilibration time	120 s
Concentration NPs	10 mg/L (Au) 50 mg/L (CuO) 100 mg/L (SiO_2 and Ami-SiO_2)
0.5x PBS	
pH	7.8 ± 0.2
Temperature	25 °C
Ionic strength	83 mM
Viscosity	0.8508 cP
Macromolecules/NOM present	none

Fig S1. The shake flask method for octanol water partitioning performed using Au NPs. Particles were visually observed to partition to the aqueous phase.

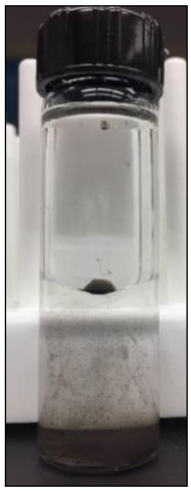

CuO NPs added to octanol and water after 24 hrs

CuO NPs mixed with octanol and water for 4 hrs

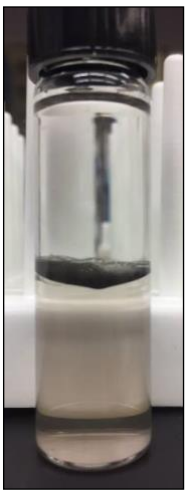

Liquid phases allowed to separate for 3 hrs

1 mL sample taken from each liquid phase

Fig S2. The shake flask octanol-water partitioning method performed with CuO NPs. NPs are visually observed to sit at the octanol-water interface.

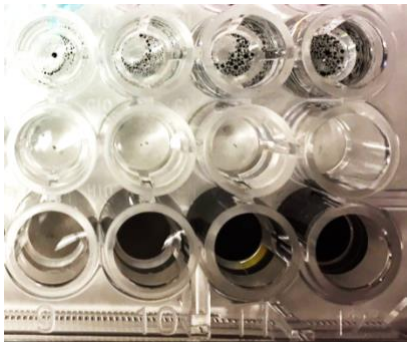

octanol

water

Fig S3. CuO NPs suspended in octanol and water. A standard curve could not be performed to quantify CuO concentration in octanol because NPs could not be uniformly dispersed.

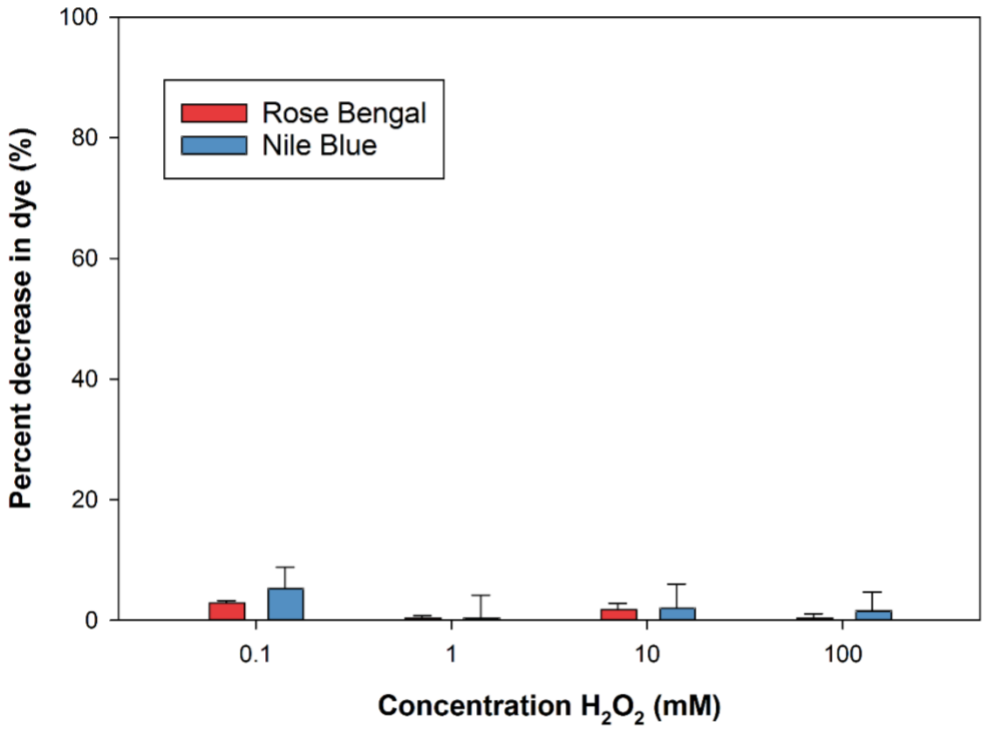

Fig S4. Percent decrease in dye concentration as a function of hydrogen peroxide concentration.

Environmental Transformations

Water samples were collected on August 13, 2018. Conductivity, pH and all other water quality parameters were measured within one day of water collection. Dye adsorption experiments were performed within three days of water collection.

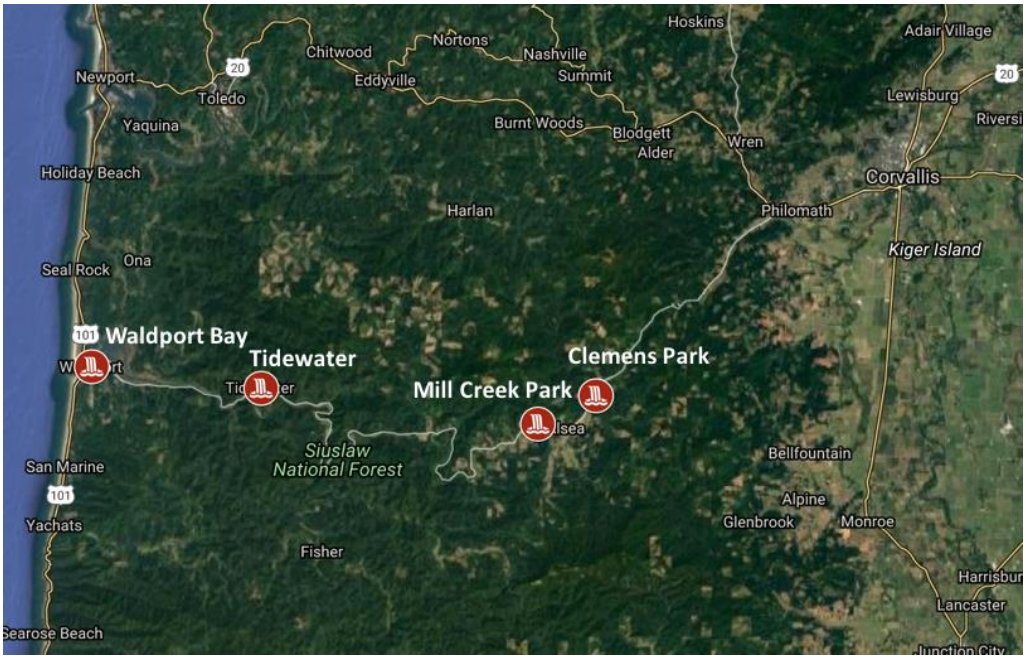

Fig S5. Water collection locations along the Alsea River Watershed.

Table S2. Water Quality Parameters.

Location	GPS Coordinates	pH	Conductivity (µS)	Alkalinity (mg/L $CaCO_3$)	Hardness (mg $CaCO_3$/L)
Clemens Park	44°24'34" N 123°34'4" W	7.84	110	29	58
Mill Creek Park	44°23'5" N 123°37'24" W	7.75	90	24	36
Tidewater	44°23'5" N 123°37'26" W	7.31	13000	24	1030
Waldport Bay	44°25'54" N 123°3'32" W	7.69	53500	38	3960

TiO_2 NPs (10 mg/L) were suspended in each of the water samples and incubated for 90 minutes. Hydrodynamic diameter and zeta potential measurements were subsequently performed using a Malvern Zetasizer (Nano ZS, Malvern Instruments, Worcestershire, UK).

Table S3. Hydrodynamic diameter (HDD) and zeta potential for 10 mg/L TiO_2 in each water source.

Location	HDD (nm)	Zeta Potential (mV)
MQ H_2O	1223	-8.58
Clemens Park	3354	-15.3
Mill Creek Park	413	-7.4
Tidewater	2398	-15.8
Waldport Bay	2256	-7

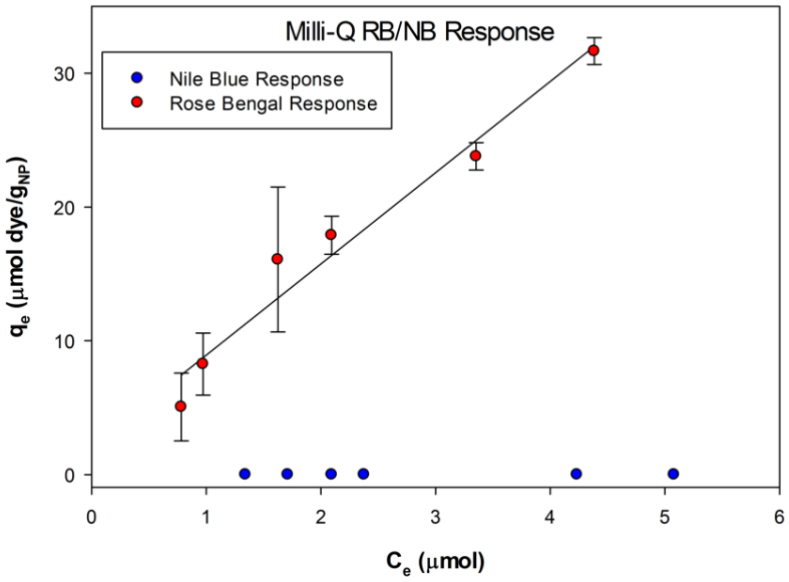

Fig S6. 250 mg/L TiO2 P-25 NPs in Milli-Q Water with Nile Blue and Rose Bengal (0-15 µM). Nile Blue did not adsorb to the surface, but Rose Bengal was fit to a linear isotherm model (R^2=0.96).

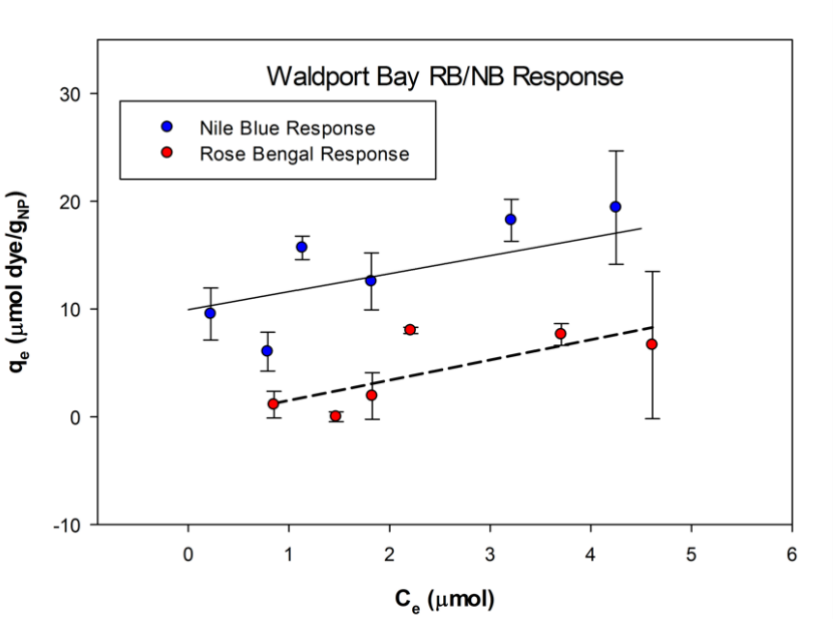

Fig S7. 250 mg/L TiO2 P-25 NPs in water from Waldport Bay with Nile Blue and Rose Bengal (0-15 µM). Linear isotherm models were used to measure adsorption of Nile Blue (blue) and Rose Bengal (red) dyes (R_2=0.7 and R_2=0.55, respectively).

Figures S6 and S7 compare responses of TiO_2 NPs in Milli-Q water and after incubation in Waldport Bay water, respectively. Significant differences ($p \leq 0.05$) between both $k_{lin,RB}$ and $k_{lin,NB}$ for each treatment of NPs was observed. This indicates environmental transformations caused differences in hydrophobicity measurements and can be measured. The transformations were observed even after NPs were removed from the natural water and resuspended in MQ.

This method was performed in all water samples and the linear adsorption parameters are shown in Table S4.

Table S4. Linear adsorption parameters for adsorption of RB and NB to 250 mg/L TiO_2 in natural waters.

Water Collection Location	**$k_{lin,RB}$**	**$k_{lin,NB}$**	**Hydrophobicity Ratio ($k_{lin,RB}$/ $k_{lin,NB}$)**	**Log Hydrophobicity Ratio**
Clemens	0.001	0.1075	9.212×10^{-3}	-2.035
Mill Creek	0.001	0.001	1	0
Tidewater	1.1978	0.3949	3.033	0.482
Waldport	1.8360	2.8178	0.651	-0.186
MQ	6.9059	0.001	6906	3.839

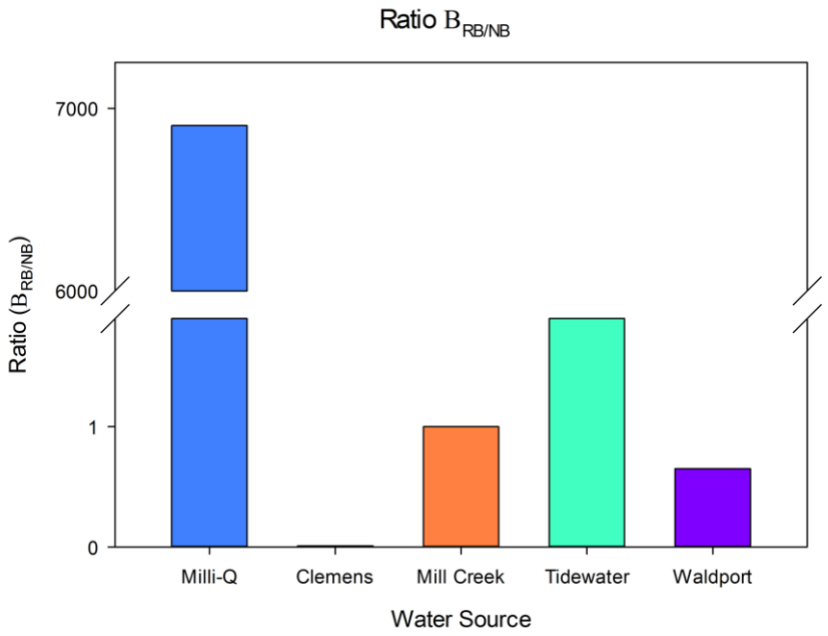

Fig S8. Hydrophobicity ratio based on linear adsorption isotherms for 250 mg/L TiO_2 in various natural waters. A higher ratio indicates a more hydrophobic particle surface. Here, β, represents the linear adsorption parameter k_{lin}.

Conclusions

Significant transformation ($p \leq 0.05$) in hydrophobicity of TiO_2 P-25 NPs from control Milli-Q water laboratory tests were found after incubation in all four natural water samples (Fig. S8.). Most notably, a substantial hydrophilic response was observed in Waldport Bay waters; this represents a drastic shift from the distinct hydrophobic response of TiO_2 in Milli-Q water (Fig. S6., Fig. S7.). Implications of this observed transformation from exclusively hydrophobic NPs to NPs that undergo hydrophilic adsorption include potential differences in mechanisms for natural organic matter (NOM) surface adsorption, suspension stability, and organismal uptake (56), (3). While TiO_2 expressed significant hydrophilic response in Waldport Bay waters, hydrophobic dye adsorption still occurred (Fig. S7.). This continued hydrophobic response could be linked to the core hydrophobicity of TiO_2 despite transformations in the nanoparticle's surface chemistry (3). Additionally, NP agglomeration, which is probable according to HDD and zeta potential measurements, impacts available NP surface area, potentially altering hydrophobic interactions leading to the observed dual response (Table S3). It is currently unclear how the simultaneous hydrophobic and hydrophilic response would impact cellular uptake, but it is known that hydrophobic NPs experience heightened uptake compared to hydrophilic counterparts (3). This suggests less cellular uptake of these environmentally transformed TiO_2 NPs when compared to pristine TiO_2 NPs. However, further research on environmentally transformed NP hydrophobicity and its effect on cellular uptake is required to draw substantial conclusions.

Additionally, it is possible that dye adsorption to hydrophobic active sites on the surface of TiO_2 NPs was blocked by adsorbed dissolved organic matter (DOM), decreasing the observed hydrophobic response. Adsorption of organic material onto NP surfaces in natural environments impacts the behavior of the NP and has the potential to modify the behavior of the adsorbed

material. These dual and interconnected transformations suggest that released NPs are both contaminants and contaminant carriers (56).

Future Work

These observed environmental transformations after incubation in natural waters demonstrate distinct and currently unpredictable differences in NP behavior between laboratory and natural settings. Significant changes in physicochemical properties, including hydrophobicity, have the potential to alter a NPs organism uptake, toxicity, and fate and transport. Therefore, understanding the natural factors that influence these transformations can provide valuable guidance for predictive modeling after NP release into the environment. Factors within river systems that can impact NP transformation include water quality parameters like salinity, pH, and natural organic matter (NOM) concentrations. Additional research is required to quantify the impact of specific parameters on NP environmental transformations.

Furthermore, temporal tests with varying tide levels should be completed to describe the complex environment that NPs interact with as they travel from source water to ocean. Tide cycles influence the salinity of water within an estuarine system, which can cause NP agglomeration and effectively reduce the relative surface area available for redox reactions and for adsorbing chemicals on the NP surface (57).

Understanding the environmental transformation of NPs after release into the environment is a critical component of more accurately modelling their fate and transport. Broadening knowledge beyond pristine laboratory settings is essential for predicting and preparing for the potential impacts of NPs on the environment, organisms, and ultimately humans.

References

1. Finizio A, Vighi M, Sandroni D. Determination of n-octanol/water partition coefficient (Kow) of pesticide critical review and comparison of methods. Chemosphere. 1997;34(1):131–61.

2. Li Y, Chen X, Gu N. Computational Investigation of Interaction between Nanoparticles and Membranes : Hydrophobic / Hydrophilic Effect. J Phys Chem B. 2008;112(51):16647–53.

3. Bai X, Wang S, Yan X, Zhou H, Zhan J, Liu S, et al. Regulation of Cell Uptake and Cytotoxicity by Nanoparticle Core under the Controlled Shape, Size, and Surface Chemistries. ACS Nano. 2020 Jan 28;14(1):289–302.

4. Kulacki KJ, Cardinale BJ. Effects of Nano-Titanium Dioxide on Freshwater Algal Population Dynamics. Bansal V, editor. PLoS ONE. 2012 Oct 10;7(10):e47130.

5. Stark WJ, Stoessel PR, Wohlleben W, Hafner A. Industrial applications of nanoparticles. Chem Soc Rev. 2015;44(16):5793–805.

6. BCCResearch. Global Markets for Nanocomposites, Nanoparticles, Nanoclays, and Nanotubes. 2017.

7. Alvarez PJJ, Colvin V, Lead J, Stone V. Research priorities to advance eco-responsible nanotechnology. ACS Nano. 2009;3(7):1616–9.

8. Lowry G V., Hotze EM, Bernhardt ES, Dionysiou DD, Pedersen JA, Wiesner MR, et al. Environmental Occurrences, Behavior, Fate, and Ecological Effects of Nanomaterials: An Introduction to the Special Series. J Environ Qual. 2010;39(6):1867.

9. Xia T, Zhao Y, Sager T, George S, Pokhrel S, Li N, et al. Decreased dissolution of ZnO by iron doping yields nanoparticles with reduced toxicity in the rodent lung and zebrafish embryos. ACS Nano. 2011;5(2):1223–35.

10. Li S, Zhai S, Liu Y, Zhou H, Wu J, Jiao Q, et al. Experimental modulation and computational model of nano-hydrophobicity. Biomaterials. 2015;52(1):312–7.

11. Xia XR, Monteiro-riviere N a, Mathur S, Song X, Xiao L, Oldenburg SJ, et al. Mapping the Surface Adsorption Forces of Nanomaterials in Biological Systems Mapping the Surface Adsorption Forces of Nanomaterials in Biological Systems. 2011;(11):9074–81.

12. Zhu M, Nie G, Meng H, Xia T, Nel A, Zhao Y. Physicochemical properties determine nanomaterial cellular uptake, transport, and fate. Acc Chem Res. 2013;46(3):622–31.

13. Mudunkotuwa IA, Pettibone JM, Grassian VH. Environmental implications of nanoparticle aging in the processing and fate of copper-based nanomaterials. Environ Sci Technol. 2012;46(13):7001–10.

14. Moyano DF, Saha K, Prakash G, Yan B, Kong H, Yazdani M, et al. Fabrication of corona-free nanoparticles with tunable hydrophobicity. ACS Nano. 2014;8(7):6748–55.

15. Kim ST, Saha K, Kim C, Rotello VM. The role of surface functionality in determining nanoparticle cytotoxicity. Acc Chem Res. 2013;46(3):681–91.

16. Aggarwal P, Hall JB, McLeland CB, Dobrovolskaia MA, McNeil SE. Nanoparticle interaction with plasma proteins as it relates to particle biodistribution, biocompatibility and therapeutic efficacy. Adv Drug Deliv Rev. 2009;61(6):428–37.

17. Hou W-C, Moghadam BY, Corredor C, Westerhoff P, Posner JD. Distribution of Functionalized Gold Nanoparticles between Water and Lipid Bilayers as Model Cell Membranes. Environ Sci Technol. 2012;46(3):1869–76.

18. Topuz E, Sigg L, Talinli I. A systematic evaluation of agglomeration of Ag and TiO2 nanoparticles under freshwater relevant conditions. Environ Pollut. 2014;193:37–44.

19. Muller RH, Ruhl D, Luck M, Paulke Bernd-R. Influence of Fluorescent Labelling of Polystyrene Particles on Phagocytic Uptake, Surface Hydrophobicity, and Plasma Protein Adsorption. Pharm Res. 1997;14(1):18–24.

20. Song JE, Phenrat T, Marinakos S, Xiao Y, Liu J, Wiesner MR, et al. Hydrophobic interactions increase attachment of gum arabic- and PVP-coated Ag nanoparticles to hydrophobic surfaces. Environ Sci Technol. 2011;45:5988–95.

21. Praetorius A, Tufenkji N, Goss K-U, Scheringer M, von der Kammer F, Elimelech M. The road to nowhere: equilibrium partition coefficients for nanoparticles. Environ Sci Nano. 2014;1(4):317–23.

22. Thomas DN, Judd SJ, Fawcett N. Flocculation modelling: A review. Water Res. 1999;33(7):1579–92.

23. Barton LE, Therezien M, Auffan M, Bottero J-Y, Wiesner MR. Theory and Methodology for Determining Nanoparticle Affinity for Heteroaggregation in Environmental Matrices Using Batch Measurements. Environ Eng Sci. 2014;31(7):421–7.

24. Geitner NK, O'Brien NJ, Turner AA, Cummins EJ, Wiesner MR. Measuring Nanoparticle Attachment Efficiency in Complex Systems. Environ Sci Technol. 2017;51(22):13288–94.

25. Praetorius A, Labille JJ, Scheringer M, Thill A, Hungerbühler K, Bottero JY, et al. Heteroaggregation of titanium dioxide nanoparticles with model natural colloids under environmentally relevant conditions. Environ Sci Technol. 2014;48(18):10690–8.

26. Praetorius A, Scheringer M, Hungerbühler K. Development of environmental fate models for engineered nanoparticles - A case study of TiO 2 nanoparticles in the rhine river. Environ Sci Technol. 2012;46(12):6705–13.

27. Azimi G, Dhiman R, Kwon H-M, Paxson AT, Varanasi KK. Hydrophobicity of rare-earth oxide ceramics. Nat Mater. 2013;12(4):315–20.

28. Xiao Y, Wiesner MR. Characterization of surface hydrophobicity of engineered nanoparticles. J Hazard Mater. 2012;215–216(216):146–51.

29. Arnaudov LN, Cayre OJ, Stuart AC, Stoyanov D, Stuart MAC, Stoyanov SD, et al. Measuring the three-phase contact angle of nanoparticles at fluid interfaces. Phys Chem Chem Phys. 2010;12(2):328–31.

30. Deak A, Hild E, Kovacs AL, Horvolgyi Z. Contact angle determination of nanoparticles: film balance and scanning angle reflectometry studies. Phys Chem Chem Phys. 2007;9(48):6359–70.

31. Maestro A, Guzmán E, Ortega F, Rubio RG. Contact angle of micro- and nanoparticles at fluid interfaces. Curr Opin Colloid Interface Sci. 2014;19(4):355–67.

32. Meylan WIMM, Oward PHHH, Oethling ROSB. Improved Method for Estimating Water Solubility From Octanol / Water Partition Coefficient. Environ Toxicol Chem. 1999;18(4):664–72.

33. Jafvert CT, Kulkarni PP. Buckminsterfullerene's (C 60) Octanol-Water Partition Coefficient (K ow) and Aqueous Solubility. Environ Sci Technol. 2008;42(765):5945–50.

34. Petersen EJ, Huang Q, Weber WJ. Relevance of octanol-water distribution measurements to the potential ecological uptake of multi-walled carbon nanotubes. Environ Toxicol Chem. 2010;29(5):1106–12.

35. Hristovski KD, Westerhoff PK, Posner JD. Octanol-water distribution of engineered nanomaterials. J Environ Sci Health - Part ToxicHazardous Subst Environ Eng. 2011;46(6):636–47.

36. Queiroz JA, Tomaz CT, Cabral JMS. Hydrophobic interaction chromatography of proteins. J Biotechnol. 2001;87(2):143–59.

37. Carstensen H, Muller BW, Muller RH. Adsorption of ethoxylated surfactants on nanoparticles. I. Characterization by hydrophobic interaction chromatography. Int J Pharm. 1991;67(1):29–37.

38. Jones MC, Jones SA, Riffo-Vasquez Y, Spina D, Hoffman E, Morgan A, et al. Quantitative assessment of nanoparticle surface hydrophobicity and its influence on pulmonary biocompatibility. J Controlled Release. 2014;183(1):94–104.

39. Rieux A Des, Ragnarsson EGE, Gullberg E, Préat V, Schneider YJ, Artursson P. Transport of nanoparticles across an in vitro model of the human intestinal follicle associated epithelium. Eur J Pharm Sci. 2005;25:455–65.

40. Doktorovova S, Shegokar R, Martins-Lopes P, Silva AM, Lopes CM, Müller RH, et al. Modified Rose Bengal assay for surface hydrophobicity evaluation of cationic solid lipid nanoparticles (cSLN). Eur J Pharm Sci. 2012;45(5):606–12.

41. OECD. OECD guideline for the testing of chemicals: partition coefficient (n-octanol/water): shake flask method. Giudance. 1995;107(July):1–4.

42. Keller AA, Wang H, Zhou D, Lenihan HS, Cheer G, Cardinale BJ, et al. Stability and Aggregation of Metal Oxide Nanoparticles in Natural Aqueous Matrices. Env Sci Technol. 2010;44(6):1962–7.

43. Aksoy BS, Yarar B. Natural hydrophobicity of native gold flakes and their flotation under different conditions. In: Dobby GS, Rao SR, editors. Proceedings of the International Symposium on Processing of Complex Ores. Halifax; 1989. p. 19–27.

44. Smith T. The hydrophilic nature of a clean gold surface. J Colloid Interface Sci. 1980;75(1):51–5.

45. ChemAxon. Chemicalize [Internet]. ChemAxon. 2017 [cited 2018 Mar 31]. Available from: https://chemicalize.com/#/

46. Liu X, Jiang Z, Li J, Zhang Z, Ren L. Super-hydrophobic property of nano-sized cupric oxide films. Surf Coat Technol. 2010;204(20):3200–4.

47. Vencalek BE, Laughton SN, Spielman-Sun E, Rodrigues SM, Unrine JM, Lowry G V., et al. In Situ Measurement of CuO and Cu(OH)2 Nanoparticle Dissolution Rates in Quiescent Freshwater Mesocosms. Environ Sci Technol Lett. 2016;3(10):375–80.

48. Tufenkji N, Elimelech M. Breakdown of colloid filtration theory: Role of the secondary energy minimum and surface charge heterogeneities. Langmuir. 2005;21(3):841–52.

49. Chowdhury I, Hong Y, Honda RJ, Walker SL. Mechanisms of TiO2 nanoparticle transport in porous media: Role of solution chemistry, nanoparticle concentration, and flowrate. J Colloid Interface Sci. 2011;360(2):548–55.

50. Li X, Scheibe TD, Johnson WP. Apparent decreases in colloid deposition rate coefficients with distance of transport under unfavorable deposition conditions: A general phenomenon. Environ Sci Technol. 2004;38(21):5616–25.

51. Ayawei N, Ebelegi AN, Wankasi D. Modelling and Interpretation of Adsorption Isotherms Modelling and Interpretation of Adsorption Isotherms. Hindawi J Chem. 2017;1–11.

52. Cestari AR, Vieira EFS, Vieira GS, Almeida LE. Aggregation and adsorption of reactive dyes in the presence of an anionic surfactant on mesoporous aminopropyl silica. J Colloid Interface Sci. 2007;309(2):402–11.

53. Velmurugan P, Shim J, Oh BT. Removal of anionic dye using amine-functionalized mesoporous hollow shells prepared from corn cob silica. Res Chem Intermed. 2016;42(6):5937–50.

54. Wu F, Hicks AL. Estimating human exposure to titanium dioxide from personal care products through a social survey approach. Integr Environ Assess Manag. 2019;107.

55. Hu Y, Guo T, Ye X, Li Q, Guo M, Liu H, et al. Dye adsorption by resins: Effect of ionic strength on hydrophobic and electrostatic interactions. Chem Eng J. 2013;228:392–7.

56. Abbas Q, Yousaf B, Amina, Ali MU, Munir MAM, El-Naggar A, et al. Transformation pathways and fate of engineered nanoparticles (ENPs) in distinct interactive environmental compartments: A review. Environ Int. 2020 May 1;138:105646.

57. Levard C, Hotze EM, Lowry GV, Brown GE. Environmental Transformations of Silver Nanoparticles: Impact on Stability and Toxicity. Environ Sci Technol. 2012 Jul 3;46(13):6900–14.